ELSEVIER

Astroparticle Physics 2 (1994) 103–116

Astroparticle Physics

Single muon angular distributions observed in the LVD particle astrophysics experiment

M. Aglietta [s], B. Alpat [p], E.D. Alyea [h,j], P. Antonioli [s], G. Anzivino [g], G. Badino [s], Y. Ban [e], G. Bari [a], M. Basile [a], A. Benelli [a], V.S. Berezinsky [m], L. Bergamasco [s], R. Bertoni [s], S. Bianco [g], A. Bizzeti [f], A. Bosco [h], G.Brugnola [a], G. Bruni [a], Y. Cao [e], G. Cara Romeo [a], R. Casaccia [g], C. Castagnoli [s], A. Castellina [s], K. Chen [e], R. Chen [e], J.A. Chinellato [c], L. Cifarelli [a], F. Cindolo [a], G. Cini [s], S. Cong [e], A. Contin [a], V.L. Dadykin [m], M. Dardo [s], A. De Silva [b], S. De Pasquale [g], M. Deutsch [k], L.G. Dos Santos [c], R.I. Enikeev [m], D. Fabbri [g], F.L. Fabbri [g], W. Fulgione [s], P. Galeotti [s], M. Gatta [g], P. Ghia [s], P. Giusti [a], F. Grianti [t], S. Gu [e], Y. Guo [k], E.S. Hafen [k,l], P. Haridas [k], D. Hungerford [g], G. Iacobucci [a], N. Inoue [q], F.F. Khalchukov [m], E.V. Korolkova [m], P.V. Kortchaguin [m], V.B. Kortchaguin [m], V.A. Kudryavtsev [m], G. Landi [f], K. Lau [i], X. Lin [e], M. Lindozzi [g], L. Lu [e], M. Luvisetto [a], J. Ma [e], Z. Ma [e], G. Maccarrone [a], A.S. Malguin [m], Z. Mao [e], M.A. Markov [m], T. Massam [a], B. Mayes [i], N. Mengotti Silva [c], A. Misaki [q], B. Monteleoni [f], C. Morello [s], J. Moromisato [ℓ], R. Nania [a], G. Navarra [s], L. Panaro [s], D. Parks [i], P.G. Pelfer [f], L. Periale [s], P. Picchi [s], L. Pinsky [i], I.A. Pless [k], M. Pu [e], J. Pyrlik [i], J. Qiu [e], V.G. Ryasny [m], O.G. Ryazhskaya [m], O. Saavedra [s], K.Saitoh [r], D. Sanders [i], G. Sartorelli [a], S. Sarwar [g], D. Shen [e], N. Taborgna [h], V.P. Talochkin [m], H. Tang [e,f], J. Tang [k], W. Tian [e], G.C. Trinchero [s], A. Turtelli [c], I. Uman [p], P. Vallania [s], M. Ventura [g], S. Vernetto [s], E. von Goeler [ℓ], L. Votano [g], T. Wada [n], F. Wang [e], H. Wang [e], S. Wang [e], R. Weinstein [i], M. Widgoff [b], L. Xu [k], Z. Xu [e], V.F. Yakushev [m], I. Yamamoto [o], A. Zallo [g], G.T. Zatsepin [m], X. Zhou [e], Q. Zhu [e], X. Zhu [e], B. Zhuang [e], A. Zichichi [d]

[a] *University of Bologna and INFN-Bologna, Italy*
[b] *Brown University, Providence, RI 02912, USA*
[c] *University of Campinas, Campinas, Brazil*
[d] *CERN, Geneva, Switzerland*
[e] *Chinese Academy of Science, Beijing, China and I.C.S.C. World Laboratory*
[f] *University of Firenze and INFN-Firenze, Italy*
[g] *INFN/LNF, Frascati, Italy*
[h] *INFN/LNGS, Assergi, Italy*
[i] *University of Houston, Houston, TX 77004, USA*
[j] *Indiana University, Bloomington, IN 47405, USA*
[k] *Massachusetts Institute of Technology, Cambridge, MA 02139, USA*
[ℓ] *Northeastern University, Boston, MA 02115, USA*
[m] *INR Russian Academy of Sciences, Moscow, Russia*
[n] *Okayama University, Okayama, Japan*

0927-6505/94/$7.00 © 1994 Elsevier Science B.V. All rights reserved
SSDI 0927-6505(94)00008-Q

[o] Okayama University of Science, Okayama, Japan
[p] University of Perugia and INFN-Perugia, Italy
[q] Saitama University, Saitama, Japan
[r] Ashikaga Institute of Technology, Ashikaga, Japan
[s] Institute of Cosmo-Geophysics, CNR, Torino, Italy, University of Torino and INFN-Torino, Italy
[t] University of Urbino, and INFN-Firenze, Italy

Received 21 December 1993

Abstract

The first angular distribution data from 5547 hours of operation of the LVD detector are presented. The technique of track reconstruction is described. A total of 452 657 single muons were reconstructed for this period. The data are acceptance corrected in our final plots. The total single muon flux (the total flux from above impinging on a sphere of unit cross sectional area) in the Gran Sasso Laboratory is 1.03 muons per hour per square meter. The total flux crossing a unit horizontal area from above is 0.79 muons per hour per square meter. The acceptance-corrected intensity at $\cos\theta = 1$ is 0.349 muons per hour per square meter per steradian (9.7×10^{-9} muons per second per square centimeter per steradian). We present, for the first time from Gran Sasso Laboratory, data at near-horizontal zenith angles.

1. Introduction

The Large Volume Detector (LVD) experiment [1] is located in the INFN Gran Sasso Laboratory [2] at a depth of $\sim$ 3600 meters of water equivalent. The apparatus consists of a streamer tube tracking system interleaved with a large volume of liquid scintillator and its support structure, which acts as a passive absorber. It is thus a high precision tracking calorimeter with the major part of its volume sensitive and with sensitive elements uniformly distributed throughout [3]. Of the five towers which will constitute the complete LVD, one has been operational since June 1992. We report in this paper on the tracking system and muon data taken during the first year of operation.

It is noteworthy that our data extend to a nearly horizontal zenith angle. This is the first time such data are available from the Gran Sasso Laboratory. We also note that the angular distributions presented have been acceptance corrected.

Near-horizontal underground muons could provide information on several particle physics and astrophysics questions [4–7]. One of the unique features of the Gran Sasso laboratory is the rich mountain structure; below $\cos\theta = 0.5$ there is a wide range of slant depths at each zenith angle, and a wide range of zenith angles at each slant depth. This will enable separating angle dependent effects from energy dependent effects in a way not possible in other laboratories.

For example, we can measure the zenith angle distribution of the π and K components and compare to expectations from atmospheric showering models [5]; extract the prompt muon flux and the overall charm cross section [4,5,7]; and observe the neutrinos interacting in the rock [6]. Limits on neutrino oscillations and neutrinos from AGN's [4] can be set from a study of this latter process.

Some of the richness of the mountain structure can be seen even at angles more near the vertical. However, notice that restricting observations to $\cos\theta$ values greater than 0.3 [8] does not permit [9] observations in the interesting region of slant depth suggested elsewhere [4–7]. The LVD is designed to examine this interesting region with

[1] Coresponding author: E.S. Hafen, Massachusetts Institute of Technology, Cambridge, MA 02139, USA.

high precision.

Section 2 contains the detector description and the basic features of the tracking system. In Section 3 the track reconstruction program and the overall acceptance and detection efficiency are described. In Section 4 the acceptance and efficiency corrected single muon angular distributions, dominated by the mountain structure in the immediate vicinity of the laboratory, are presented. Section 5 contains our conclusions.

2. Detector description

The completed LVD will contain 190 modules grouped into 5 identical aligned towers of 38 modules each. The single LVD tower has a surface area of 660 m^2 and an acceptance of 1768 m^2 sr for an isotropic flux. At present we have completed the first tower, whose main characteristics are summarized in Table 1, the scintillator component in Table 2, and the tracking component in Table 3.

2.1. Tower and module descriptions

A module consists of a steel carrier containing 8 liquid scintillation counters, each viewed from the top by 3 photomultipliers. Each module also contains a double layer of limited streamer tubes [10] mounted on an L-shaped structure. This structure is attached to the bottom and to one vertical side of a steel carrier as shown in Figs. 1 and 2. Each module contains about 9.6 tons of scintillator and 9.5 tons of steel.

Table 1
Main characteristics of LVD first tower.

Characteristic	Value
surface area	660 m^2
acceptance for isotropic flux	1768 m^2 sr
length × width × height	7 m × 13 m × 12 m
scintillator mass	368 tons
iron mass (scintillator containers and carrier)	360 tons
tracking channels	17408
streamer tubes	2928
tracking spatial resolution	$\simeq$ 1 cm
angular resolution	$\leq$ 4 mrad
energy resolution	15% at 10 MeV

As shown in Fig. 3, the modules in a tower form 5 columns of 7 (side columns) or 8 (center columns) modules each, with the 1.14 m high modules separated vertically by 0.36 m. The 2.20 m wide columns are separated by a 0.55 m wide passageway at 4 levels for easy access to all the detector elements. To provide maximum acceptance, tracking detectors on alternate levels are wider and extend under the passageways.

2.2. Tracking system

The tracking system consists of L-shaped tracking detectors [11], each leg of which contains two layers of limited streamer tubes. The basic tube element is an 8-cell (9×9 mm^2 active cross-section area) open profile constructed of 1 mm thick extruded PVC coated with graphite. A 100 μm diameter silvered Be-Cu anode wire is stretched along the central position of each cell, supported every 50 cm by a plastic spacer, and soldered at the two ends to printed circuit boards. The profile structure is enclosed by a PVC sleeve and end caps with connections for high voltage and gas flow. Below and running parallel to the streamer tube wires are $\sim$ 4 cm wide pickup strips (x-strips), while above and running perpendicular to the wires are pickup strips (y-strips) of similar width, to provide bidimensional information about an ionizing particle's impact point. The y-strips extend across both the horizontal and the vertical sides of the tracking detector in an L shape. The two tracking detector layers are separated from the steel carrier by ground planes.

The tubes of the two layers (and hence also the x-strips) are staggered by 1.5 cell widths or approximately half the strip spacing, while the y-strips of the two layers are staggered by half the strip spacing. The relative locations of the two staggered layers of streamer tubes, their supporting structure ("panel"), and the scintillation counters can be seen in the cross section of a module shown in Fig. 2. The staggered double layer of streamer tubes and the staggered layers of orthogonal readout strips in the tracking sys-

Table 2
First tower scintillation counters.

Characteristic	Value
liquid scintillation counters	304
length × width × height (each counter)	1.5 m × 1.0 m × 1.0 m
PM tubes (3/counter)	15 cm diameter (FEU-49B)
composition (average)	C_nH_{2n} ($\langle n \rangle = 9.6$) + 1 g/ℓ PPO + 0.03 g/ℓ POPOP
density	~ 0.8 g/cm^3
scintillator mass (each counter)	~ 1.2 tons
sensitivity (average)	15 photoelectrons/counter MeV
attenuation length	> 15 m at $\lambda = 420$ nm

Table 3
First tower LVD tracking system.

Characteristic	Value
tracking detectors	38
limited streamer tubes (LST)	8 cells
cell size (including 1 mm cell walls)	1 cm × 1 cm × 6.3 m
wires	100 μm diameter silvered BeCu
operating voltage	4.7 kV
gas mixture before 19 November 1992	30% Ar + 70% isobutane
gas mixture after 19 November 1992	88% CO_2 + 2% Ar + 10% isobutane
number of LSTs tracking per detector per layer	vertical: 12; horizontal: 24 (narrow) or 30 (wide)
pickup strip width	~ 4 cm
number of strips per tracking detector per layer	152 ($y = \perp$ wire), 24 (vertical $x = \parallel$ wire) 48 (narrow horizontal $x = \parallel$ wire), or 60 (wide horizontal $x = \parallel$ wire)
vertical active area/tracking detector	6.21 m × 1.04 m
narrow horizontal (22) active area/tracking detector	6.21 m × 2.07 m
wide horizontal (16) active area/tracking detector	6.21 m × 2.52 m

tem yield an effective strip width of 2 cm with no dead space, high overall track detection efficiency, and an angular resolution better than 4 milliradians [12].

2.3. Tracking data acquisition

A block diagram of the tracking data acquisition system is shown in Fig. 4. The 448 (narrow tracking detectors) or 472 (wide tracking detectors) pickup strips of each tracking detector are read out by a digital streamer tube readout system which consists of a chain of sixteen 32-channel Thomson-SGS front-end cards, a line driver card and a Camac based Streamer Tube Readout Card (STROC) designed at Padua University [13], as well as a pattern generator card.

The front-end cards of the tracking detectors are daisy chained to the line driver at one end to facilitate the transmission of data to the STROCs and on the other end to a pattern generator card which is read out on each trigger to ensure the integrity of the data. In the front-end cards, the pickup strip signals are first discriminated and then stored in a one-shot for 2.5 microseconds. The one-shots are connected to a 32 bit parallel in–serial out shift register which is loaded and read out when a trigger occurs. The discriminated x-strip signals are also OR-ed together by a trigger fan-in card on each tracking detector to form 4 signals (horizontal and vertical, inner and outer layers) which are then used by the tracking trigger system.

The tracking trigger is formed by OR-ing the

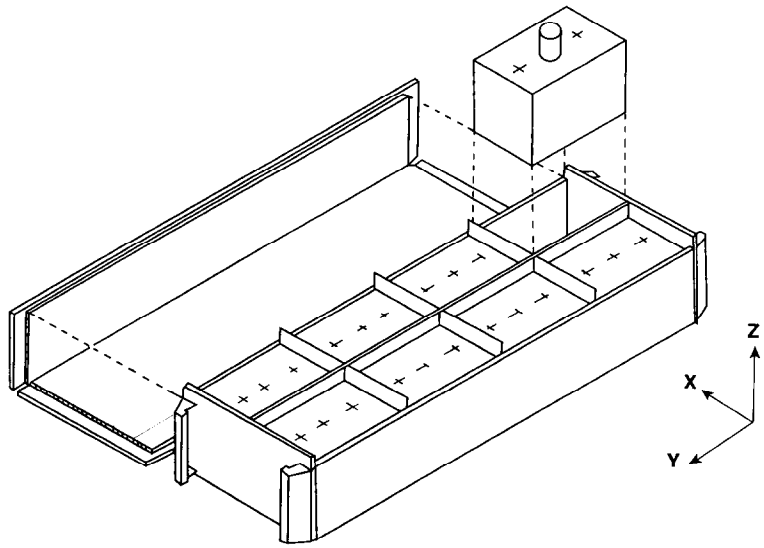

Fig. 1. LVD steel carrier with tracking detector and scintillation counters.

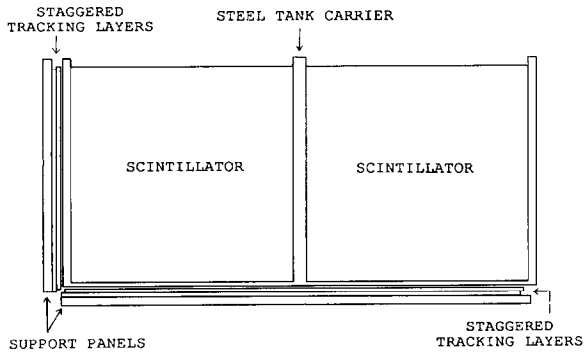

Fig. 2. End view of LVD steel carrier with tracking detector and scintillation counters.

4 signal layers (horizontal and vertical, inner and outer) from the various tracking detectors to form 10 vertical and 16 horizontal tower layer signals and by requiring the time coincidence of at least 4 of them. The scintillation counter system trigger is formed when any counter has an energy deposit above a preset threshold (4–7 MeV). These two triggers are OR-ed to form the master LVD trigger. This master trigger is fanned out to all the STROCs and thence to all front-end cards. On reception of the trigger signals, the one-shot output levels are loaded into the shift registers. The shift registers are then read out serially by the STROC, which can handle 8 separate daisy chains in parallel, and stored

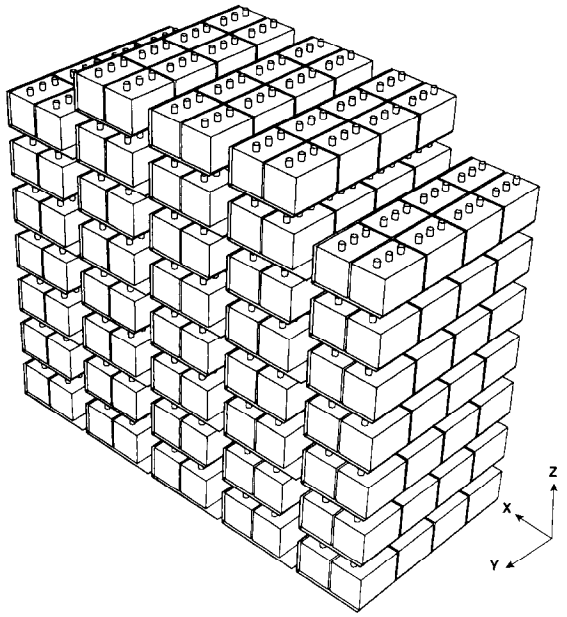

Fig. 3. LVD tower 1 front view (looking west).

in memory with the zeroes suppressed. When this is completed, the STROCs are read out by a Starburst J-11 front-end processor which sends the data to a microVAX to be written on a disk [14].

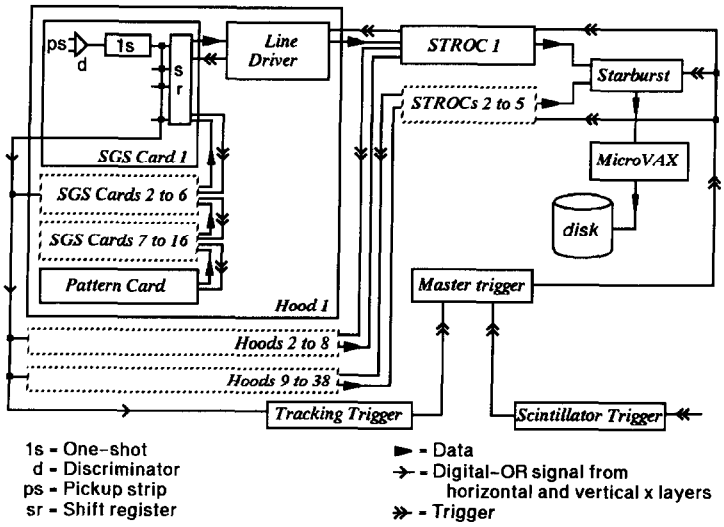

Fig. 4. Tracking data acquisition system.

3. Analysis

The LVD is a multipurpose detector, with a loose hardware trigger designed to accommodate many physics topics. Consequently, a software trigger must be imposed for any specific study. A single muon passing through a module will in general strike 1 or 2 scintillation counters and 2 or 4 layers of streamer tubes. The signal produced in the tubes by the traversing muon is picked up by nearby ("hit") x-strips and y-strips. A set of adjacent hit x-strips or y-strips is termed a "cluster". Accordingly a "LEG" software trigger occurs when at least one x-strip cluster in the horizontal portion or in the vertical portion of a tracking detector is hit, as well as at least one y-strip cluster. This is the minimum amount of information needed to define a "point", which is a set of 2–4 clusters in a leg, containing at least one x-strip cluster and at least one y-strip cluster.

Tracks are reconstructed as straight lines using the tracking data only, which means that at least two legs must be struck, and the LEG condition satisfied on both. To reduce the number of accidental LEG coincidences, we require that energy be deposited in a scintillation counter in each accepted event. These requirements motivate the selection of runs and of events given in Section 3.3.

3.1. Track reconstruction program

Most fixed target or colliding beam experiments have an event vertex, which simplifies the problem of track reconstruction. The LVD experiment has no such constraint on track reconstruction. In addition, the LVD tracking detectors have an L-shaped geometry which further complicates the track reconstruction problem. It was therefore necessary to write a pattern recognition and track reconstruction program specifically designed for the LVD experiment. The track reconstruction program PIPR [12] (Particle Information and Pattern Recogniton) has undergone extensive testing, and was used to process the data presented in this paper.

The strategy used by PIPR is:

(1) select an x-strip cluster and a y-strip cluster to form a master point;

(2) select another x-strip cluster and a y-strip cluster, on a different leg from the master point, to form a slave point and thus determine a line;

(3) add clusters along this trajectory;

(4) do a 3-dimensional fit [15] to the selected elements;

(5) store satisfactory track candidates;
(6) repeat (2)–(5) with other slave points;
(7) after all appropriate slaves have been tried, repeat (1)–(6) until all suitable master points have been tried;
(8) select the "best" set of candidates.

If the event processing time limit is exceeded during the search, it is terminated for that event by immediately proceeding to (8). The best set of candidates is selected from those found within the time limit. A processing time cut of 200 seconds was used as a compromise between reconstructing high multiplicity tracks in a single pass and spending too much time searching for tracks within showers. Additional conditions were applied to the reconstructed tracks, as detailed in Section 3.3, to assure that the tracks corresponded to real muons.

3.2. Monte Carlo

The simple Monte Carlo used to test the general software package was modified to calculate the acceptance corrections. Straight lines (1.5×10^7) were generated on a sphere corresponding to 20 160 m^2 sr, containing the entire five towers of the future LVD. Any live elements in the first tower intercepted by a line were turned "on". The fraction of Monte Carlo events with at least one element turned on was 8.77%, corresponding to an acceptance for an istropic flux of 1768 m^2 sr, very close to the estimated geometric acceptance of 1700 m^2 sr for one tower.

The acceptance of the LVD detector as a function of $\cos\theta$ and ϕ depends on the trigger strategy, detector efficiencies, and the operational fraction of the detector. All of these effects must be included in the Monte Carlo.

The inefficiencies for the data sample studied, in order of their effect on the distributions considered, were:

(1) losses due to the 1 mm plastic walls of the 9×9 mm^2 square (active area) gas cells of the streamer tubes;
(2) dead streamer tubes;
(3) tracking detectors not yet operational;
(4) dead discriminators;
(5) y-strip inefficiencies at the tube ends;
(6) misalignment of the steel carriers to which the tracking detectors are attached;
(7) electronic inefficiencies and noise.

The effect of the streamer tube walls can be estimated geometrically. The effects of the dead streamer tubes and the not-yet-operational tracking detectors can be accounted for precisely as can the effect of the dead discriminators and the inefficiency of the y-strips at the tube ends. The misalignment of the steel carriers to which the tracking detectors are attached is not known precisely, nor are the electronic inefficiency and noise; their effects must be estimated by comparison with the actual data.

We find that all of these losses together are sufficiently small that in general only one or two clusters are lost of the four clusters possible in a leg traversed by a muon. This means that these inefficiencies have only a minor effect on the acceptance for a reconstructed track which satisfies a three LEG trigger (TK-LEG3 trigger).

As a check on the validity of the efficiency modifications to the Monte Carlo, we compared the distributions of the cluster number along the tracks for the Monte Carlo samples to that for the data sample, using a TK-LEG3 trigger. Since each leg traversed contains four sense strip layers, the number of clusters along a track should be a multiple of four if the efficiency were 100%. Fig. 5a shows the distribution of clusters with the TK-LEG3 trigger for the Monte Carlo with no inefficiencies applied. Except for the edge effect where layers are staggered, the distribution does indeed show the expected multiple of four. Fig. 5b shows the same Monte Carlo cluster distribution after imposing the inefficiencies discussed above. This should be compared to the cluster distribution for our analyzed data with a TK-LEG3 trigger imposed, shown in Fig. 5c. Figs. 5b and 5c are quite similar. We also checked that the total acceptance-corrected flux was independent of the trigger chosen. The differences among the acceptance-corrected totals were about 1%, providing an estimate of the systematic effects of the Monte Carlo assumptions. Hence we believe we understand our detector inefficiencies.

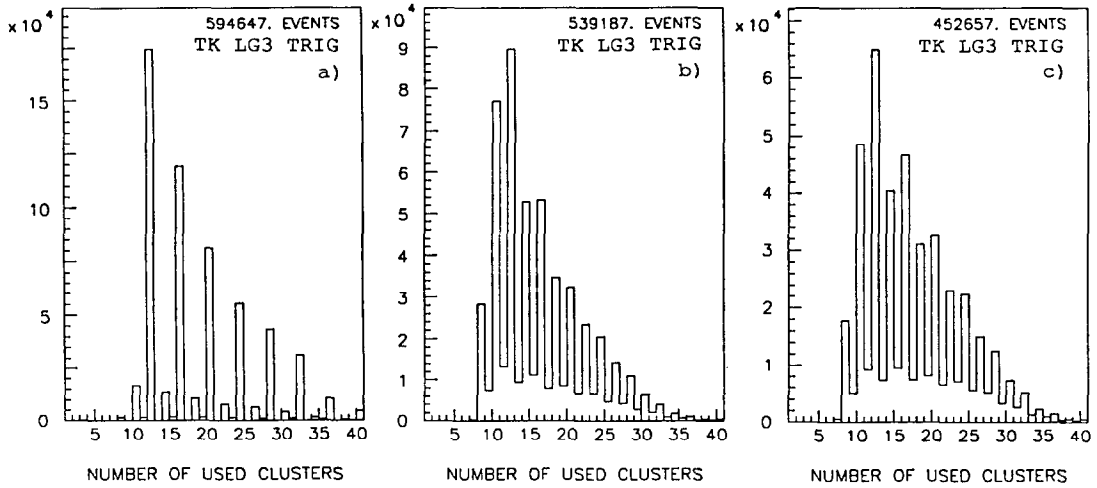

Fig. 5. Number of used clusters for (a) 100% efficient Monte Carlo; (b) Monte Carlo with detector inefficiencies; (c) single muon sample. Note that the average number of layers of gas cells traversed is about 10 (i.e., 20 clusters). Hence the 1 mm plastic cell wall, which leads to a 10% layer inefficiency, causes at least one of the layers to be lost, shifting part of each peak at a multiple of 4 clusters (a) to multiples of 2 clusters (b, c).

3.3. Event selection

For the study discussed in this paper we have used data taken between 17 June and 19 November 1992, and between 12 January and 30 May 1993. Selections were made according to the following criteria.

A. Run criteria:

(1) duration of the run greater than 10 minutes;

(2) at least 24 of the 38 tracking detectors triggered during the run;

(2) at least 200 of the 304 scintillation counters triggered during the run;

(3) EV-LEG2 trigger (defined below) average rate for the run greater than 0.2 per minute.

B. Event criteria:

(1) LEG condition satisfied on at least two legs (minimum needed for a straight line);

(2) both x-strip layers triggered on at least one leg (rejects random background);

(3) at least one scintillation counter triggered in the tower (assures that a charged particle existed in the event);

(4) no tracking detector with more than 80% of its strips hit (assure that the tracking system was working properly).

Conditions (1)–(3) constitute the "two-LEG software trigger on events", or EV-LEG2 trigger.

For the runs included in this study, the EV-LEG2 trigger average rate was 1.87 per minute. Reconstructed tracks from PIPR were analyzed for only those events which passed the event and run criteria. The detailed effects of our criteria are given in the following paragraphs.

In the 5547 hours of live time included in the data sample, 1194180 events satisfied the requirements that at least two LEGs were hit and that at least one leg had both x-strips hit (criteria B.1 and B.2). Of these events, 52.3% (624353) satisfied the requirement that at least one scintillator counter was hit in the event (criterion B.3). Finally, 99.4% of the remaining events satisfied the requirement that no tracking detector had more than 80% of its strips hit (3734 failed; criteria B.4). The event selection procedure produced 620619 software trigger events whose PIPR results were analyzed. PIPR found at least one muon candidate in 99.2% (615912) of these events. After reconstruction, two criteria were applied to each reconstructed track to remove very short tracks and tracks lying within

a tracking layer. All tracks with fewer than five clusters were rejected, as were any tracks that had more than one point in the same layer. Only 0.4% (2549) and 0.2% (1077), respectively, of the events were rejected for these two reasons. This left 612 286 events of all multiplicities. Finally, we accepted only single muon events (584 951 events) where the reconstructed track contained at least three LEGs (452 657 events). As discussed later, an additional 27 events are discarded in regions of low acceptance, and therefore we are left with a total of 452 630 events in the final data sample.

The Monte Carlo data, generated with an isotropic distribution, were analyzed with the same event selection criteria as the experimental data. Since the two data samples have very different initial angular distributions, and no physics processes were included in the Monte Carlo, the effect of the various criteria should be very different for the two samples. However, for the record, we report the detailed results of the Monte Carlo of the simulated isotropic distribution. Fifteen million Monte Carlo events were generated uniformly on a sphere corresponding to 20 160 m^2 steradians. Conditions B.1 and B.2 were passed by 5.3% of the events (790 606). Only 1.1% of these failed condition B.3 (781 599 passed). PIPR found no track in only 0.063% of the remainder, yielding 781 108 events, all reconstructed as single muons. Requiring at least five clusters on a track and no more than one point of a track lying within a plane removed 0.002% (13) and 0.02% (182), respectively, of the reconstructed Monte Carlo tracks. Requiring a track to have at least three LEGs rejected 31.0% of the remaining Monte Carlo events for a final total of 539 187 events. This corresponds to an acceptance for an isotropic distribution of 725 m^2 steradians for a TK-LEG3 trigger.

To check the numerical effect of the efficiency corrections discussed above, the Monte Carlo data were also processed with none of the inefficiencies used above. This analysis yielded an acceptance of 799 m^2 steradians for an isotropic distribution with a TK-LEG3 trigger applied. That is, applying estimates of the detector inefficiencies results in a 10% correction to an isotropic distribution with a TK-LEG3 trigger. Applying the acceptances determined from this Monte Carlo without inefficiencies yields a total number of events for the observed anisotropic distribution with a TK-LEG3 trigger which is 7% lower than the result using acceptances determined from the more realistic Monte Carlo. Unless explicitly stated otherwise, the efficiency-corrected Monte Carlo and the acceptance corrections derived from it are used in this paper.

4. Results

Only reconstructed tracks which pass the selection criteria described in the previous section are included in the angular distributions discussed in this paper. The distributions presented in this section are given in the LVD coordinate system. The final acceptance-corrected distribution is given in the geographic coordinate system as well.

4.1. Coordinate systems

The LVD hall and the LVD y-axis are oriented approximately southeast. Track reconstruction is performed in the frame of reference defined by the shape of the LVD detector.

The origin of this frame is at the lowest northernmost steel carrier corner. The vertical z-axis running up the corner of the tower crosses the northeastern corners of seven horizontal double-layer tracking planes. The x-axis is the horizontal axis which runs across the smaller dimension of the modules and is perpendicular to the five columns of modules and to the vertical tracking planes. The y-axis lies along the long bottom northeastern edge of the lowest northeastern steel carrier. With these choices the x-axis points almost southwest and the y-axis points southeast. The axis orientations are shown in Figs. 1 and 3.

The spherical coordinates used have the polar angle measured from the z-axis and the azimuthal angle measured counter clockwise from the x-axis. This LVD reference system is used for

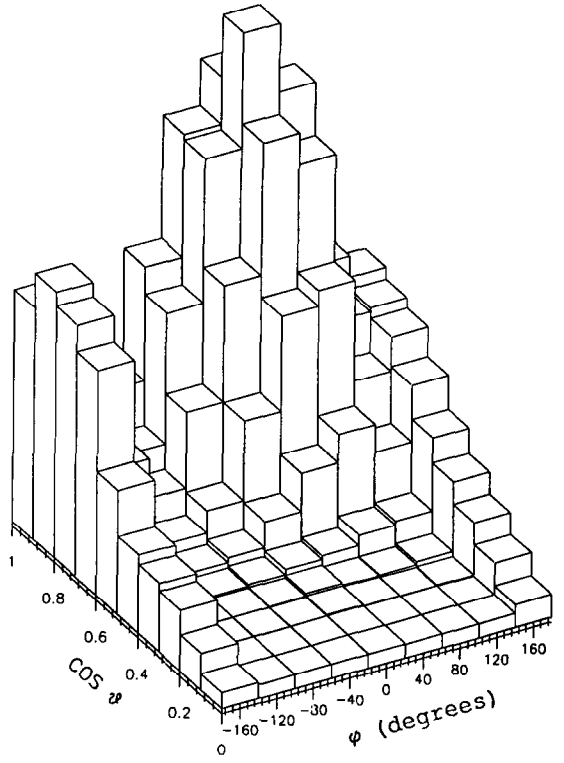

Fig. 6. Lego plot of the number of single muon events as a function of azimuth and $\cos\theta$. There are 11 589 events in the bin at $\cos\theta = 1$ and $\phi = -180$.

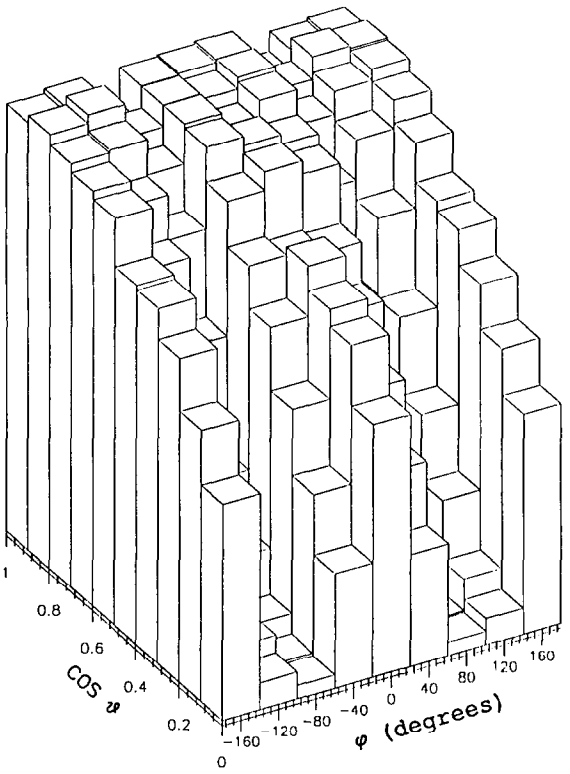

Fig. 7. Lego plot of LVD acceptance (1 tower) from the Monte Carlo with detector inefficiencies, as a function of muon azimuth and $\cos\theta$. Note that the acceptance from $\cos\theta = -1$ to $\cos\theta = +1$ has been folded about 0. The total acceptance in the bin at $\cos\theta = 1$ and $\phi = -180$ is 11.6 m^2 sr.

Figs. 8, 9. The azimuthal angle of geographical North is $-141.6°$ in the LVD reference system.

In Fig. 10 data are displayed in the geographical reference frame with the azimuthal angle measured clockwise from North. The relationship between the geographical azimuth angle and the LVD azimuth angle is:

$$\phi(\text{geographical}) = 218.4° - \phi(\text{LVD}).$$

4.2. *Single muon angular distributions*

Fig. 6 shows a lego plot of the number of single muon events as a function of azimuth and $\cos\theta$ in the LVD reference system. Most of the muons arrive at the LVD through the plateau near $\cos\theta = 0.9$ and $\phi = 40°$. A substantial number of muons also come through the valley between the two major sets of mountain peaks, near $|\phi| = 180°$. These muons arrive along the LVD's x-axis.

Fig. 7 shows a lego plot of the LVD acceptance (1 tower) for a TK-LEG3 trigger. This plot is derived from the Monte Carlo with detector inefficiencies as a function of muon azimuth and $\cos\theta$ in the LVD reference system. Note that the LVD acceptance for a TK-LEG3 trigger extends to $\cos\theta = 0$ along the $\pm x$-axes at $\phi = 0$ and $\pm 180°$, and is zero on only 8% of the Monte Carlo sphere, in regions near the $\pm y$-axes where there are few muons because the slant depths are large. For the distributions discussed, events occurring in regions where the acceptance is less than 2% are not included. This discards an additional 27 events, concentrated on less than 1% of the sphere, within the region

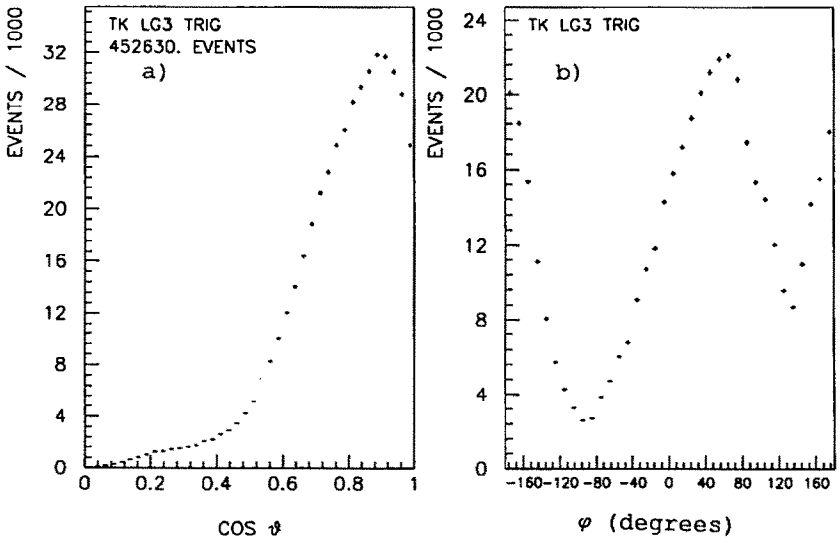

Fig. 8. Single muon angular distributions: (a) polar angle; (b) azimuthal angle.

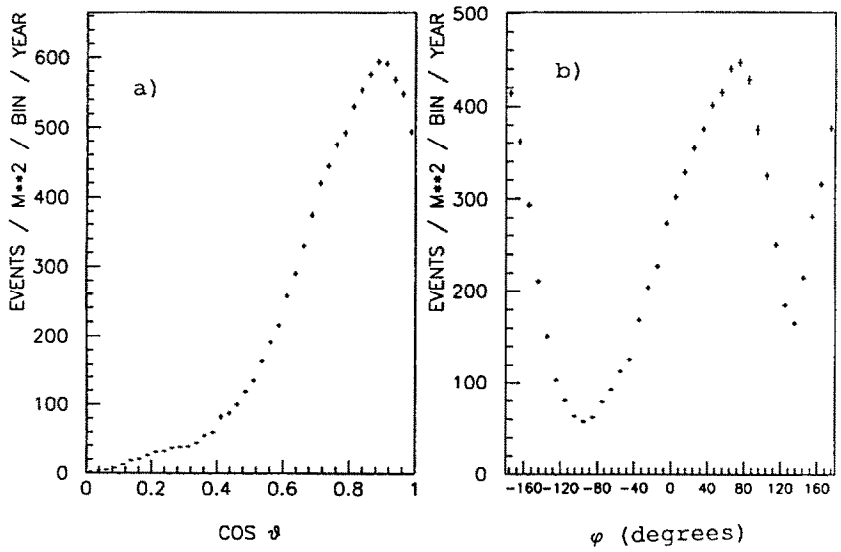

Fig. 9. Acceptance-corrected single muon angular distributions in the LVD reference system: (a) polar angle; (b) azimuthal angle. The integral of each of these distributions is 9062 events / m^2 yr.

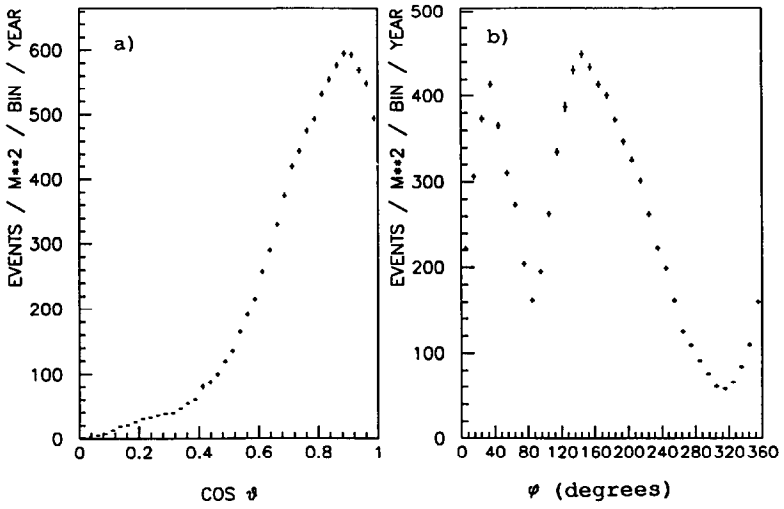

Fig. 10. Acceptance-corrected single muon angular distributions determined in the geographic reference system: (a) polar angle; (b) azimuthal angle.

bounded by $0.25 \leq \cos\theta \leq 0.375$ and $80° \leq \phi \leq 100°$. Only a few events are discarded in the symmetric region near $\phi = -90°$; the mountain is much thicker in that direction.

Fig. 8a shows the single muon $\cos\theta$ distribution and Fig. 8b is the azimuthal distribution in the LVD reference system. Because the acceptance is small only in regions of little data, the dips shown in the ϕ distribution are primarily due to the absorption of muons by the nearby mountain ranges.

4.3. Acceptance-corrected distributions

The single muon intensity is defined as the acceptance-corrected number of single muons per unit cross sectional area per unit solid angle per unit time. The total single muon flux from above is the single muon intensity integrated over solid angle; it corresponds to the number of events which would be seen by a 100% efficient spherical detector of unit cross sectional area in one unit of time. The total single muon flux crossing unit horizontal area from above is the integral of the product of the single muon intensity with $\cos\theta$; it corresponds to the number of events incident on a 100% efficient horizontal planar detector of unit area in one unit of time from above. Note that all observed flux is assumed to be downward.

Fig. 9a shows the acceptance-corrected $\cos\theta$ flux distribution and Fig. 9b shows the corresponding azimuthal distribution in the LVD coordinate system. The acceptance corrections and the acceptance-corrected flux distributions were also determined in the geographic coordinate system. Fig. 10a shows the resulting acceptance-corrected $\cos\theta$ flux distribution and Fig. 10b is the corresponding azimuthal distribution in the geographic coordinate system.

A lego plot of the acceptance-corrected intensity is shown in Fig. 11. The acceptance-corrected intensity has a maximum in the bin $0.85 \leq \cos\theta \leq 0.875$ and $40° \leq \phi \leq 50°$, where it has the value 7248 events/m^2 sr yr.

The number of single muons passing through the LVD in 5547 hours of operation is 452 630. This corresponds to an acceptance-corrected total single muon flux of $9062 \pm 18 \pm 90$ muons/m^2 yr. The first error is statistical. The second error is an estimate of the systematic effects of the modeling of the detector inefficiencies, based on the differences between the acceptance-corrected fluxes for different triggers. The acceptance-corrected total single muon flux crossing a unit horizontal area per unit time from above is

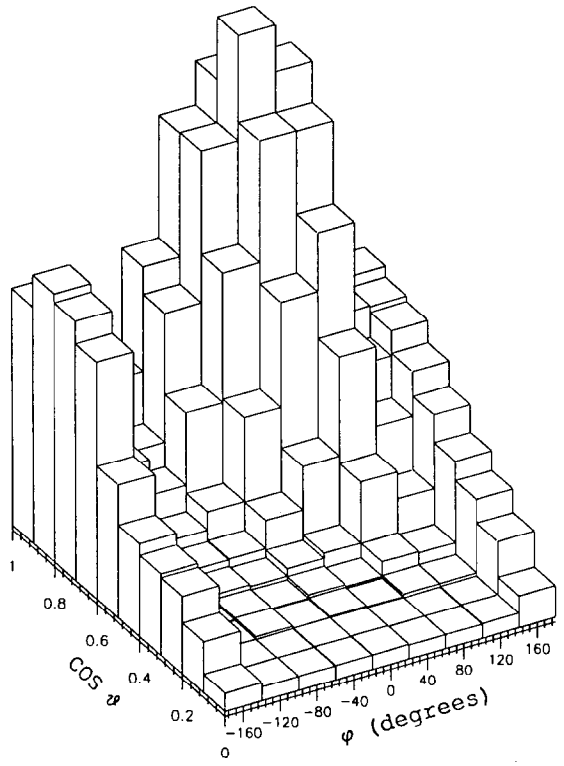

Fig. 11. Lego plot of the acceptance corrected single muon intensity as a function of azimuth and $\cos\theta$. The intensity in the bin at $\cos\theta = 1$ and $\phi = -180$ is 3146/m^2 sr yr.

$6886 \pm 13 \pm 90$ muons/m^2 yr.

5. Conclusions

The first tower of the LVD experiment has been operational since June 1992. We have measured the angular distributions of the incident muons using the data of the first year of operation. These distributions have been fully acceptance corrected. For the first time data in the $\cos\theta = 0$ range are available from the Gran Sasso Laboratory.

We have measured the total single muon flux (the total flux from above impinging on a sphere of unit cross sectional area) to be $1.034 \pm 0.002 \pm 0.010$ muons/m^2 h. The total muon flux crossing a unit horizontal area from above is $0.786 \pm 0.002 \pm 0.010$ muons/m^2 h. The first error is statistical and the second error is systematic. The acceptance-corrected intensity at $\cos\theta = 1$ is 3060 ± 25 events/m^2 sr yr (9.7×10^{-9} cm^{-2} sr^{-1} s^{-1}).

Data acquisition in the first of the five planned towers is continuing. Construction of the second tower is almost complete.

Among the single muon projects in progress are measurement of the zenith angle distribution of the π and K components and comparison to expectations from atmospheric showering models, as well as the extraction of the prompt muon flux, the overall charm cross section, and the flux of neutrinos interacting in the rock. We expect to set limits on neutrino oscillations and neutrinos from AGN's from a study of this latter process.

Acknowledgments

We wish to thank the staff of the Gran Sasso Laboratory for their aid and collaboration. One of the authors would like to thank L. Banks of the physics department and J. Province of Computer Services at Southwest Missouri State University for providing network access during the preparation of this document. This work was supported by the Italian Institute for Nuclear Physics (INFN) and in part by the US Department of Energy, the US National Science Foundation, and the State of Texas under its TATRP program.

References

[1] C. Alberini et al., Nuovo Cimento C 9 (1986) 237.
[2] A. Zichichi, Proceedings of GUD Workshop, Rome (Frascati), 1981 (141);
A. Zichichi, CERN EP/88-28, Invited Plenary Lecture presented at the Symposium: "Present Trends Concepts and Instruments of Particle Physics" in honor of M. Conversi's 70th birthday, Rome, 3–4 November 1987.
[3] G. Bari et al., Nucl. Instrum. Methods A 277 (1989) 11.
[4] E. Zas, F. Halzen and R.A. Vazquez, Astroparticle Physics 1 (1993) 297.
[5] T.K. Gaisser, Cosmic Rays and Particle Physics, (Cambridge University Press, Cambridge, 1990) pp. 77–84.
[6] M. F. Crouch et al., Phys Rev. D 18 (1978) 2239.

[7] C. Castagnoli et al., Nuovo Cimento A 82 (1984) 78.
[8] S. Ahlen et al., Astrophys. J. 412 (1993) 301.
[9] A. Lamanna et al., Proc. 24th Int. Cosmic Ray Conference, Calgary, 4, (1993) 391.
[10] E. Iarocci, Nucl. Instrum. Methods 217 (1983) 30.
[11] G. Anzivino et al., Nucl. Instrum. Methods A 329 (1993) 521.
[12] E. Hafen, in: Arkansas Gamma-Ray and Neutrino Workshop, eds. G. B. Yodh, D. C. Wold, and W. R. Kropp (North-Holland, Amsterdam, 1989) p. 325.
[13] A. Cavestro et al., Nucl. Instrum. Methods A 312 (1992) 571.
[14] W. Fulgione et al., IEEE Trans. Nuclear Science 36 (1989) 1635.
[15] E. Hafen, PIPR equations, APC Engineering Note 89-2 (1989) (unpublished).
[16] M. Aglietta et al., Nuovo Cimento 105A (1992) 1793.